Theory of Photon Blockade by an Optical Cavity with One Trapped Atom

K. M. Birnbaum, A. Boca, R. Miller, A. D. Boozer, T. E. Northup, and H. J. Kimble

Norman Bridge Laboratory of Physics 12-33
California Institute of Technology, Pasadena, CA 91125
(Dated: July 6, 2005)

In our recent paper [1], we reported observations of photon blockade by one atom strongly coupled to an optical cavity. In support of these measurements, here we provide an expanded discussion of the general phenomenology of photon blockade as well as of the theoretical model and results that were presented in Ref. [1]. We describe the general condition for photon blockade in terms of the transmission coefficients for photon number states. For the atom-cavity system of Ref. [1], we present the model Hamiltonian and examine the relationship of the eigenvalues to the predicted intensity correlation function. We explore the effect of different driving mechanisms on the photon statistics. We also present additional corrections to the model to describe cavity birefringence and ac-Stark shifts.

I. INTRODUCTION

The phenomenon of photon blockade, first proposed in Ref. [2] in analogy with Coulomb blockade for electrons [3, 4, 5], occurs when the absorption of a first input photon by an optical device blocks the transmission of a second one, thereby leading to nonclassical output photon statistics. Photon blockade has been predicted in many different settings [6, 7, 8, 9, 10, 11], including for a single two-level atom in cavity QED [9, 12, 13, 14]. In the latter setting, the blockade is due to the anharmonicity of the Jaynes-Cummings ladder of eigenstates [15]. If an incoming photon resonantly excites the atom-cavity system from its ground state to $|1, \pm\rangle$ (where $|n, +(-)\rangle$ denotes the n-excitation dressed state with higher (lower) energy), then a second photon at the same frequency will be detuned from either of the next steps up the ladder, i.e. from states $|2, \pm\rangle$. In the strong coupling regime [16], for which the coherent rate of evolution g_0 exceeds the dissipative rates κ and γ, this detuning will be much larger than the excited-state line widths, so that the two-excitation manifold will rarely be populated. This in turn leads to the ordered flow of photons in the transmitted field, which emerge from the cavity one at a time.

We recently reported observations of photon blockade in the light transmitted by an optical cavity containing one atom strongly coupled to the cavity field [1]. For coherent excitation at the cavity input, the photon statistics for the cavity output displayed both photon antibunching and sub-Poissonian photon statistics. However, as illustrated in Fig. 1, the multiplicity of atomic and cavity states makes our experiment considerably more complex than the simple situation described by the extended Jaynes-Cummings model with damping [9, 12, 13, 14]. In our paper [1] and the accompanying Supplemental Information [17], we presented theoretical results from an extended model that described a multistate atom coupled to two cavity modes. The relevant atomic states are the Zeeman states of a particular hyperfine transition in atomic Cesium, namely $6S_{1/2}, F = 4 \leftrightarrow 6P_{3/2}, F' = 5'$ at 852 nm. The relevant modes of the Fabry-Perot cavity are two TEM_{00} modes of the same longitudinal order but orthogonal polarizations.

Our purpose in this paper is to provide a more complete discussion of photon blockade than in Ref. [1], both by way of particular results from our model calculation and of a general framework for characterization of photon blockade, with which we begin in Section II. In Section III we turn to the details of our actual system and calculate the eigenvalue structure for a two-mode cavity coupled to an atom with multiple internal states. Here, we make explicit the coupling in the model Hamiltonian which is used to determine the eigenvalues displayed in Figure 1(b) of Ref. [1]. We also incorporate this Hamiltonian into the master equation for the damped, driven system used to compute theoretical results for transmission spectra and photon statistics, as in Figure 2(b) of Ref. [1]. In Section IV, we gain some perspective on the relevant physical mechanisms by comparing transmission spectra and photon statistics for the case of an external drive that excites the atom (rather than the cavity, as in our experiment). Section V presents an extension to our atom-cavity model which includes the effect of cavity birefringence and FORT-induced ac-Stark shifts in the atomic states. The modified cavity transmission and intensity correlation functions are presented for comparison to previous results. We also display a theoretical result for the time dependence of the intensity correlation function for comparison to our measured result in Ref. [1]. Finally, in Section VI we offer a discussion of these various results.
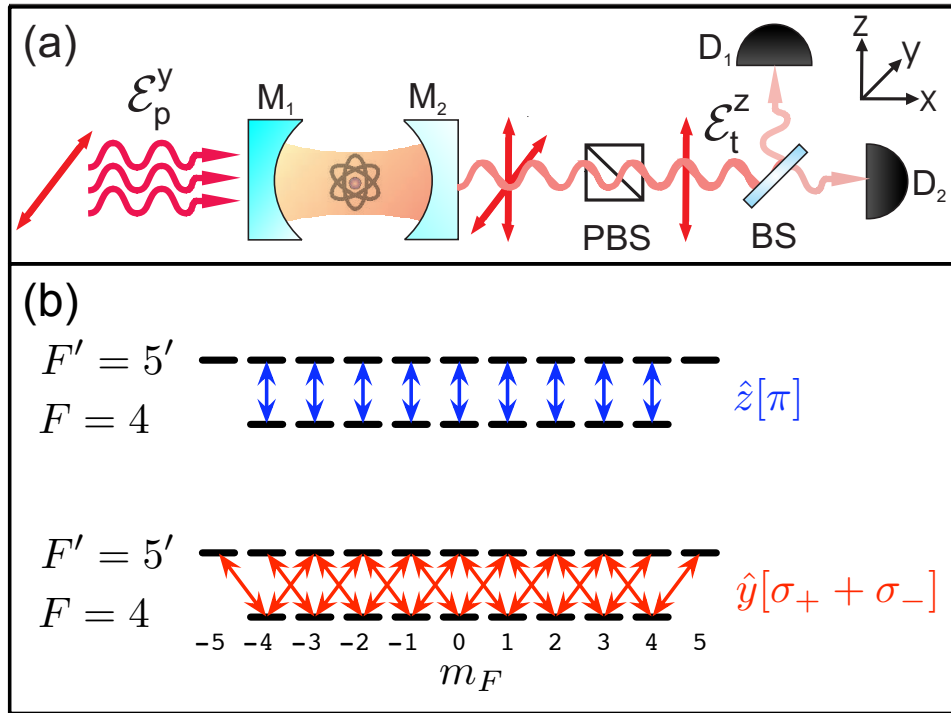
FIG. 1: (a) Diagram of the experiment of Ref. [1]; (b) illustration of the dipole operators corresponding to the two linearly polarized cavity modes. Here the atomic transition is $6S_{1/2}, F = 4 \leftrightarrow 6P_{3/2}, F' = 5$ in Cesium.

II. GENERAL CONSIDERATIONS

We begin by attempting to address the question "What is photon blockade?"[7]. Consider the following input electromagnetic field state to some "black box",

$$|\psi_{in}\rangle = \sum a_n |n\rangle . \tag{1}$$

Assume that the mapping of input to output by the black box is given by the transmission coefficients t_n for each Fock-state $|n\rangle$. The output state is then of the form

$$|\psi_{out}\rangle = \sum t_n a_n |n\rangle . \tag{2}$$

For a coherent-state input $|\alpha\rangle$, $a_n \propto \alpha^n/\sqrt{n!}$, so that

$$|\psi_{out}\rangle \propto \sum t_n \alpha^n/\sqrt{n!}|n\rangle . \tag{3}$$

A linear transfer function for the black box would be of the form $t_n \sim (t_1)^n$, so that

$$\begin{aligned}|\psi_{out}\rangle &\propto \sum (t_1\alpha)^n/\sqrt{n!}|n\rangle \\ &\propto |t_1\alpha\rangle .\end{aligned} \tag{4}$$

By contrast, a nonlinear device can modify the photon statistics in a fashion other than $|t_n| \sim |t_1|^n$. The working criterion that we adopt here for photon blockade is that the transmission coefficients $|t_n| < |t_1|^n$ for $n \geq 2$. For example, an "ideal" photon blockade device that eliminates all Fock states with $n \geq 2$ ($t_n = 0$ for $n \geq 2$) would lead to the following output for a coherent state input:

$$|\psi_{out}\rangle \propto |0\rangle + t_1\alpha|1\rangle . \tag{5}$$

Likewise, a device that produces photon pairs in abundance (and an associated large degree of photon bunching) could be specified by $|t_{n=2}| \gg |t_1|^2$, with all $t_{n>2} = 0$.

k	$\varepsilon_k^{(1)}$	$\eta_k^{(1)}$	$\varepsilon_k^{(2)}$	$\eta_k^{(2)}$
0	0	7	0	5
1	0.667	1	0.516	1
2	0.683	2	0.556	2
3	0.730	2	0.662	2
4	0.803	2	0.805	2
5	0.894	2	0.966	3
6	1	2	0.978	2
7	–	–	1.014	2
8	–	–	1.073	2
9	–	–	1.155	2
10	–	–	1.265	2
11	–	–	1.414	2

TABLE I: Numerical factors $\varepsilon_k^{(n)}$ for the eigenvalues of the Hamiltonian $H_{4\to 5'}$ in Eq. (7), together with their degeneracies $\eta_k^{(n)}$.

Of course, even in this simple setting of $in \to out$, the above discussion is incomplete since at least one additional input and output channel is required to preserve unitarity. More generally, the transformation $in \to out$ requires multiple input and output channels (e.g., polarizations for the input and output fields with a continuum of frequencies, relevant quantum degrees of freedom for the material system of the black box, etc.). These additional channels may affect the coherence of the output field, as discussed below in Section VI. Within this more complex setting, however, the conceptual framework that we suggest for identifying photon blockade still rests upon the simple intuition described above. Namely, one of the output channels should have the property that the transmission coefficients t_n satisfy $t_n < |t_1|^n$ for $n \geq 2$.

Note that the pioneering work on photon blockade based upon EIT satisfies the above criterion [2, 6, 7, 8, 9], as does resonance fluorescence from a single atom [18] and the cavity QED schemes considered in Refs. [9, 12, 13, 14]. Indeed, by the criterion stated above, most single atomic or molecular emitters function by way of photon blockade. The problem of course is that the efficiency for collecting fluorescence is typically poor. So, in addition to the more fundamental requirement $t_n < |t_1|^n$, it seems reasonable to add a second, more practical criterion related to efficiency. Photon blockade is of much less practical significance if the efficiency for the mapping of input to an output channel is negligibly small, but precisely "how small is too small" is hard to quantify and depends upon the particular application. Much of the effort related to photon blockade is directed towards maintaining the "quality" of blockade inherent in single-atom resonance fluorescence while at the same time achieving a sensibly large efficiency, which has led our group to employ an optical cavity within the setting of cavity QED, a system to which we now turn our attention.

III. EIGENVALUES OF THE ATOM-CAVITY SYSTEM

We begin this section, adapted from Ref. [17], by considering the eigenvalue structure of the atom-cavity system in the absence of damping, with the model system illustrated in Figure 1. Approximating the atom-cavity coupling as a dipole interaction, we define the atomic dipole transition operators for the $6S_{1/2}, F = 4 \to 6P_{3/2}, F' = 5'$ transition in atomic Cesium as

$$D_q = \sum_{m_F = -4}^{4} |F = 4, m_F\rangle\langle F = 4, m_F|\mu_q|F' = 5', m_F + q\rangle\langle F' = 5', m_F + q|, \quad (6)$$

where $q = \{-1, 0, 1\}$ and μ_q is the dipole operator for $\{\sigma_-, \pi, \sigma_+\}$-polarization, respectively, normalized such that for the cycling transition $\langle F = 4, m_F = 4|\mu_1|F' = 5', m_F = 5\rangle = 1$. The matrix element of the dipole operator $\langle F = 4, m_F|\mu_q|F' = 5', m'_F\rangle$ is equal to the Clebsch-Gordan coefficient for adding spin 1 to spin 4 to reach total spin 5, namely $\langle j_1 = 4, j_2 = 1; m_1 = m_F, m_2 = q|j_{total} = 5; m_{total} = m'_F\rangle$.

The Hamiltonian of a single atom coupled to a cavity with two degenerate orthogonal linear modes is

$$H_{4\to 5'} = \hbar\omega_A \sum_{m'_F = -5}^{5} |F' = 5', m'_F\rangle\langle F' = 5', m'_F| + \hbar\omega_{C_1}(a^\dagger a + b^\dagger b) \quad (7)$$
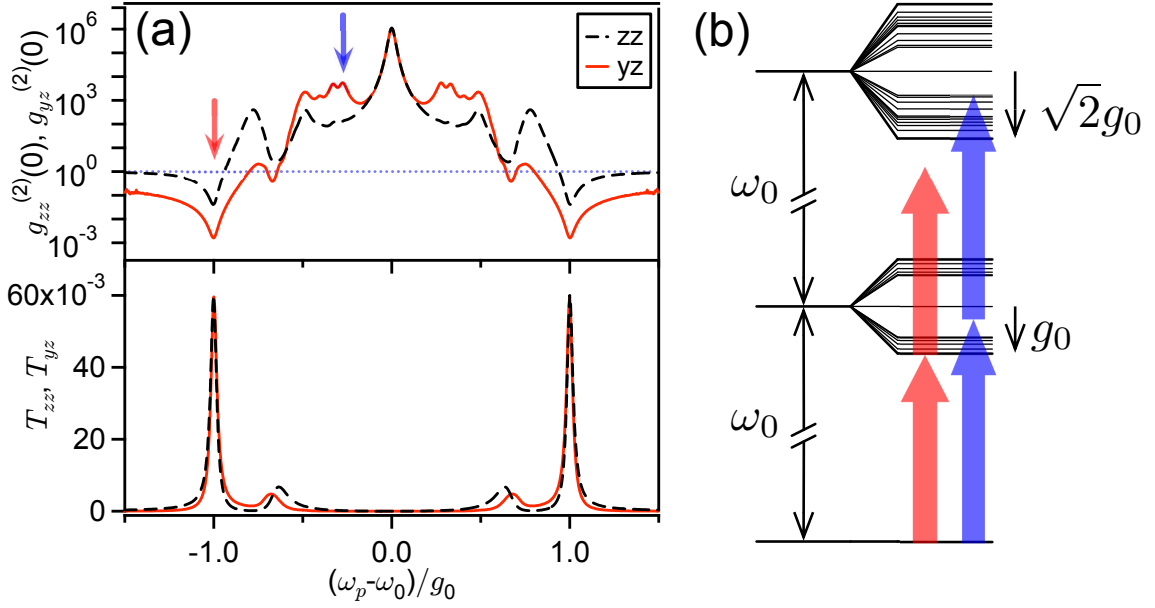$$+ \hbar g_0(a^\dagger D_0 + D_0^\dagger a + b^\dagger D_y + D_y^\dagger b)$$

FIG. 2: (a) T_{zz} and $g_{zz}^{(2)}(0)$ (dashed), and T_{yz} and $g_{yz}^{(2)}(0)$ (red) versus normalized probe detuning. We consider an $F = 4 \rightarrow F' = 5'$ transition driven by linearly polarized light in a cavity containing two modes of orthogonal polarization that are frequency-degenerate. Parameters are $(g_0, \kappa, \gamma)/2\pi = (50, 1, 1)$ MHz. The probe strength is such that the intracavity photon number on resonance without an atom is 0.05. The blue dotted line indicates $g^{(2)}(0) = 1$ for Poissonian statistics. (b) Diagram of the eigenvalue structure from Table I. Red and blue arrows denote probe frequencies indicated in (a) which lead to sub-Poissonian and super-Poissonian statistics, respectively.

where ω_A is the atomic transition frequency, ω_{C_1} is the cavity resonance frequency, and $D_y = \frac{i}{\sqrt{2}}(D_{-1} + D_{+1})$ is the dipole operator for linear polarization along the y-axis. We are using coordinates where the cavity supports $\hat{y}$ and $\hat{z}$ polarizations and $\hat{x}$ is along the cavity axis. The annihilation operator for the $\hat{z}$ ($\hat{y}$) polarized cavity mode is a (b).

Assuming $\omega_A = \omega_{C_1} \equiv \omega_0$, we find that the lowest eigenvalues of $H_{4 \rightarrow 5'}$ have a relatively simple structure. In the manifold of zero excitations, all nine eigenvalues are zero. In manifolds with n excitations, the eigenvalues are of the form $E_{n,k} = n\hbar\omega_0 + \hbar g_0 \varepsilon_k^{(n)}$, where $\varepsilon_k^{(n)}$ is a numerical factor and k is an index for distinct eigenvalues. There are 29 states in the $n = 1$ manifold, but due to degeneracy k has only 13 distinct values, $k \in \{-6, \ldots 6\}$; in the $n = 2$ manifold there are 49 states but $k \in \{-11, \ldots 11\}$. The total number of states in any manifold can be understood by considering how the excitations can be distributed among the atom and the two cavity modes. For example, in the $n = 1$ manifold, the atom can be in one of its 9 ground states ($m_F \in \{-4, \ldots 4\}$) and either cavity mode l_y or mode l_z can have one photon (giving 18 possible states), or the atom can be in one of its 11 excited states ($m_F' \in \{-5, \ldots 5\}$) while both cavity modes are in the vacuum state, yielding a total of 29 states. Table I lists numerical values for $\varepsilon_k^{(1,2)}$ as well as their respective degeneracies $\eta_k^{(1,2)}$. The numerical factors and degeneracies have the symmetries $\varepsilon_{-k}^{(n)} = -\varepsilon_k^{(n)}$ and $\eta_{-k}^{(n)} = \eta_k^{(n)}$. The resulting eigenvalues $E_{n,k}$ for $n = \{0, 1, 2\}$ are displayed in Fig. 2(b).

Although these eigenvalues are certainly not sufficient for understanding the complex dynamics associated with the full master equation, they do provide some insight into some structural aspects of the atom-cavity system. For example, the eigenvalues $\varepsilon_{\pm 6}^{(1)} = \pm 1$ correspond to the vacuum-Rabi splitting for the states $|1, \pm\rangle$ for a two-state atom coupled to a single cavity mode [cf., Fig. 1(a) of Ref. [1]]. The one-photon detunings for transitions from the $n = 1 \rightarrow n' = 2$ manifold are largest for the eigenstates associated with $\varepsilon_{\pm 6}^{(1)}$. Indeed, just as for the two-state atom with one cavity mode, transitions from the eigenstates at $\pm g_0$ have frequency detunings $\pm(2 - \sqrt{2})g_0$ relative to the nearest states in the $n' = 2$ manifold (at $\varepsilon_{\pm 11}^{(2)} = \pm\sqrt{2}$, respectively). Hence, as a function of probe frequency ω_p, the eigenvalue structure in Table I suggests that the ratio of two-photon to one-photon excitation would exhibit a minimum around $\omega_p = \omega_0 \pm g_0$, resulting in reduced values $g^{(2)}(0) < 1$ [19], which the full calculation verifies in Fig. 2(b) of Ref. [1].

For excitation to the other eigenstates in the $n = 1$ manifold, such blockade is not evidenced in Fig. 2(b) of Ref. [1]. A contributing factor suggested by the structure of eigenvalues in Table I is interference of one and two-photon excitation processes. For example, excitation at $\omega_p \simeq \omega_0 \pm g_0/4$ results in two-photon resonance for the eigenstates
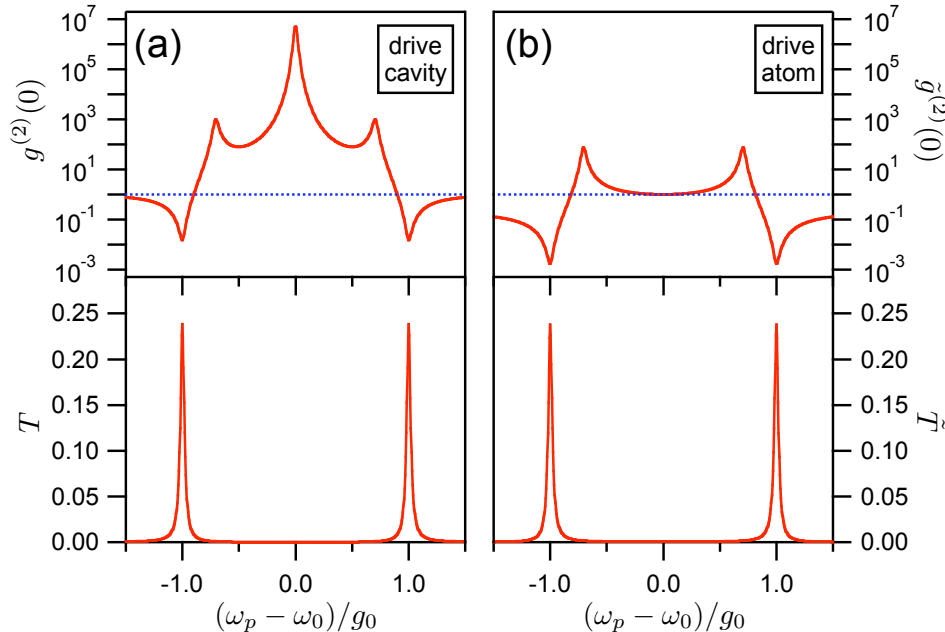
FIG. 3: Spectra and intensity correlation functions for the Jaynes-Cummings system when (a) driving the cavity T and $g^{(2)}(0)$ or (b) driving the atom $\tilde{g}^{(2)}(0)$ and $\tilde{T}$ versus normalized probe detuning. Parameters are $(g_0, \kappa, \gamma)/2\pi = (50, 1, 1)$ MHz. The probe strength is such that the intracavity photon number on resonance without an atom is 0.05 for (a), and the atomic excited state population on resonance without a cavity is 0.046 ($s/2 = 0.05$) for (b). The blue dotted lines indicates $g^{(2)}(0) = 1$ for Poissonian statistics.

associated with $\varepsilon_{\pm 1}^{(2)} \simeq \pm 0.5$, and leads to photon bunching with $g^{(2)}(0) \gg 1$ as confirmed by our full calculation of photon statistics.

Fig. 2(a) provides a global perspective of these various effects. Here, we calculate transmission spectra and intensity correlation functions analogous to those shown in Figure 2(b) of Ref. [1], but now with coherent coupling g_0 much larger than the dissipative rates (κ, γ) and well beyond what we have achieved in our experiments, $g_0/\kappa = g_0/\gamma = 50$ [20]. At $\omega_p = \omega_0 \pm g_0$, $g_{yz}^{(2)}(0) \simeq 0.002$ in evidence of the previously discussed photon blockade suggested by the eigenvalue structure in Table I. As anticipated, large photon bunching results near $\omega_p \simeq \omega_0 \pm g_0/4$ associated with the two-photon resonance to reach the eigenstates with $\varepsilon_{\pm 1}^{(2)} \simeq \pm 0.5$. Between these two extremes for the eigenvalues with the largest and smallest nonzero magnitudes $(g_0/4 \le |\omega_p - \omega_0| \le g_0)$, $g_{yz}^{(2)}(0)$ displays a complex structure involving multiple excitation pathways through states in the $n = 1$ manifold to reach states in the $n' = 2$ manifold. The extremely large peak at $\omega_p = \omega_0$ is discussed in Refs. [13, 21]. Similar calculations show that the photon blockade effect described by Fig. 2 is unaffected in its qualitative character if the atomic spontaneous decay rate γ is made much smaller than the cavity decay rate κ, although we have not set γ strictly to zero.

IV. DRIVEN ATOM

Fig. 2(b) of Ref. [1] compares the predicted photon statistics when driving the detected cavity mode ($\hat{z}$) with the statistics when driving the other cavity mode ($\hat{y}$). The driven cavity mode has photon statistics which are less strongly sub-Poissonian, an effect we hypothesize to be caused by interference between the atomic dipole radiation and the coherent drive. We will now further explore this hypothesis by considering atom-cavity systems where the driving field is directly coupled to the atom, instead of the cavity mode.

We first study the familiar Jaynes-Cummings system, a two-state atom coupled to a single mode cavity. We assume a coherent drive field made of many photons which we will treat classically. In Fig. 3, we compare the intracavity fields [22] when driving (a) the cavity and (b) the atom for $g_0/\kappa = g_0/\gamma = 50$. $T, \tilde{T}$ are proportional to the intracavity photon number, with T normalized to the empty-cavity on-resonance photon number for the driven cavity and $\tilde{T}$ normalized to half of the saturation parameter s for the driven atom. The intensity correlation function $\tilde{g}^{(2)}(0)$ of the
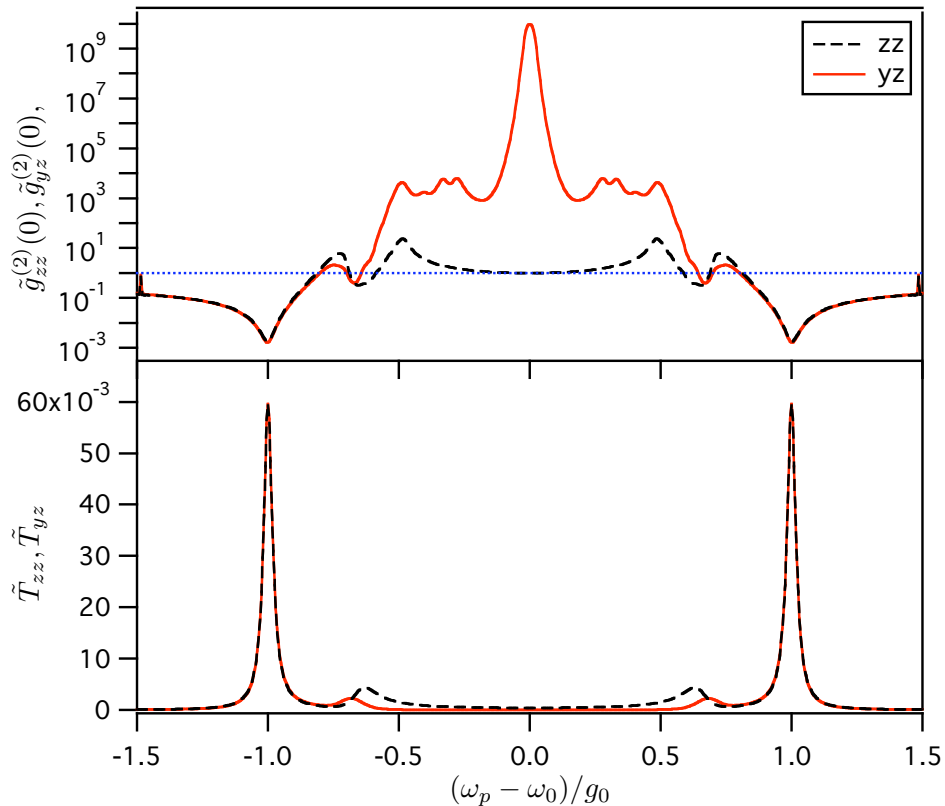
FIG. 4: Two-mode cavity coupled to a single Cs atom with direct excitation of the atom. $\tilde{T}_{zz}$ and $\tilde{g}_{zz}^{(2)}(0)$ (dashed), and $\tilde{T}_{yz}$ and $\tilde{g}_{yz}^{(2)}(0)$ (red) versus normalized probe detuning. Parameters are $(g_0, \kappa, \gamma)/2\pi = (50, 1, 1)$ MHz. The probe strength is such that the atomic excited state population on resonance without a cavity is 0.025. The blue dotted line indicates $g^{(2)}(0) = 1$ for Poissonian statistics.

system when driving the atom is much lower than $g^{(2)}(0)$ (the correlation function of the system when driving the cavity) at $\omega_p = \omega_0 \pm g_0$, with $\tilde{g}^{(2)}(0) \simeq 0.002$ and $g^{(2)}(0) \simeq 0.02$. $\tilde{g}^{(2)}(0)$ is super-Poissonian at $\omega_p = \omega_0 \pm g_0/\sqrt{2}$ due to the two-photon resonance discussed above, but lacks the large peak at $\omega_p = \omega_0$ evident in $g^{(2)}(0)$. At $\omega_p = \omega_0$ we have $\tilde{g}^{(2)}(0) \simeq 1$.

We next consider a two-mode cavity coupled to the Zeeman states of the $F = 4 \rightarrow F' = 5'$ transition of a single atom, as in Section III. We take the probe field driving the atom to be polarized along $\hat{z}$ and calculate the intracavity photon number $\tilde{T}_{zz}, \tilde{T}_{yz}$ in the $\hat{z}, \hat{y}$ modes, respectively (normalized to the drive strength as above), and the corresponding intensity correlation functions $\tilde{g}_{zz}^{(2)}(0), \tilde{g}_{yz}^{(2)}(0)$. Results of the calculations are plotted in Fig. 4 for $g_0/\kappa = g_0/\gamma = 50$. At $\omega_p = \omega_0 \pm g_0$, both $\tilde{g}_{zz}^{(2)}(0)$ and $\tilde{g}_{yz}^{(2)}(0)$ are close to $g_{yz}^{(2)}(0)$ as in Fig. 2. This supports our hypothesis that the somewhat higher value of $g_{zz}^{(2)}(0)$ at $\omega_p = \omega_0 \pm g_0$ is caused by interference with the drive field. Interestingly, though the central peak at $\omega_p = \omega_0$ is absent in $\tilde{g}_{zz}^{(2)}(0)$, as we expect in correspondence with the Jaynes-Cummings case and as implied by the usual explanation of the phenomenon as resulting from the interference of the drive field with the atomic dipole radiation, the peak in $\tilde{g}_{yz}^{(2)}(0)$ is even greater than that of $g_{zz}^{(2)}(0), g_{yz}^{(2)}(0)$. This effect may be of interest in future studies.
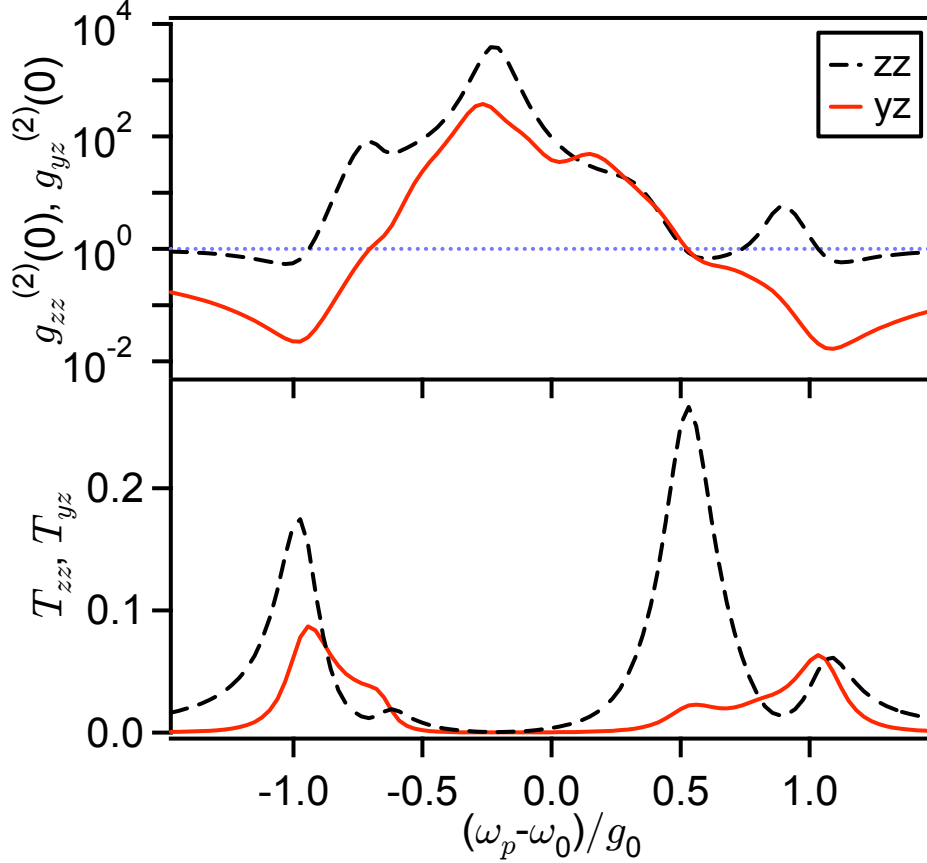
FIG. 5: T_{zz} and $g_{zz}^{(2)}(0)$ (dashed), and T_{yz} and $g_{yz}^{(2)}(0)$ (red) versus normalized probe detuning. We consider an $F = 4 \to F' = 5'$ transition (with FORT induced ac-Stark shifts) in a cavity (containing two nondegenerate modes of orthogonal polarization) driven by linearly polarized light. Parameters are $(g_0, \kappa, \gamma, \Delta\omega_{C_1}, U_0)/2\pi = (33.9, 4.1, 2.6, 4.4, -43)$ MHz, and $\omega_{C_1^z} = \omega_A \equiv \omega_0$. The probe strength is such that the intracavity photon number on resonance without an atom is 0.05. The blue dotted line indicates $g^{(2)}(0) = 1$ for Poissonian statistics.

V. BIREFRINGENCE AND STARK SHIFTS

We now consider the effects of cavity birefringence and m'_F-dependent ac-Stark shifts, expanding our previous treatment from Ref. [17]. The birefringence and ac-Stark shifts modify the Hamiltonian $H_{4 \to 5'}$ in Eq. (7) to

$$H_{full} = \sum_{m'_F=-5}^{5} \hbar\omega_{m'_F}|F' = 5', m'_F\rangle\langle F' = 5', m'_F| + \hbar\omega_{C_1^z}a^\dagger a + \hbar\omega_{C_1^y}b^\dagger b \qquad (8)$$
$$+\hbar g_0(a^\dagger D_0 + D_0^\dagger a + b^\dagger D_y + D_y^\dagger b)$$

The birefringent splitting $\Delta\omega_{C_1}$ is the difference of the resonant frequencies of the two polarization modes, $\Delta\omega_{C_1} = \omega_{C_1^z} - \omega_{C_1^y}$. The atomic excited state frequencies are given by $\omega_{m'_F} = \omega_A + U_0\beta_{m'_F}$, where ω_A is the unshifted frequency of the $F = 4 \to F' = 5'$ transition in free space, U_0 is the FORT potential, and $\beta_{m'_F}$ for the FORT wavelength of the experiment is given by $\{m'_F, \beta_{m'_F}\} = \{\pm5, 0.18\}, \{\pm4, 0.06\}, \{\pm3, -0.03\}, \{\pm2, -0.10\}, \{\pm1, -0.14\}, \{0, -0.15\}$ [23].

The effect of these corrections to the Hamiltonian on the transmitted field from the steady-state solutions to the master equation are displayed in Fig. 5, with the parameters corresponding to the experimental values from Ref. [1]. The heights and shapes of the multiplets in $T_{yz,zz}$ are modified, but the basic structure is unaffected relative to Fig. 2(b) of Ref. [1]. The structure of $g_{yz,zz}^{(2)}(0)$ is also qualitatively unchanged. The asymmetry of the plots about ω_0 is caused by the effective atom-cavity detuning (mostly due to the ac-Stark shifts). The value of $g_{yz}^{(2)}(0)$ for $\omega_p = \omega_0 - g_0$ is 0.02 (ignoring the above corrections yields $g_{yz}^{(2)}(0) \simeq 0.03$). These values are consistent with the experimental result
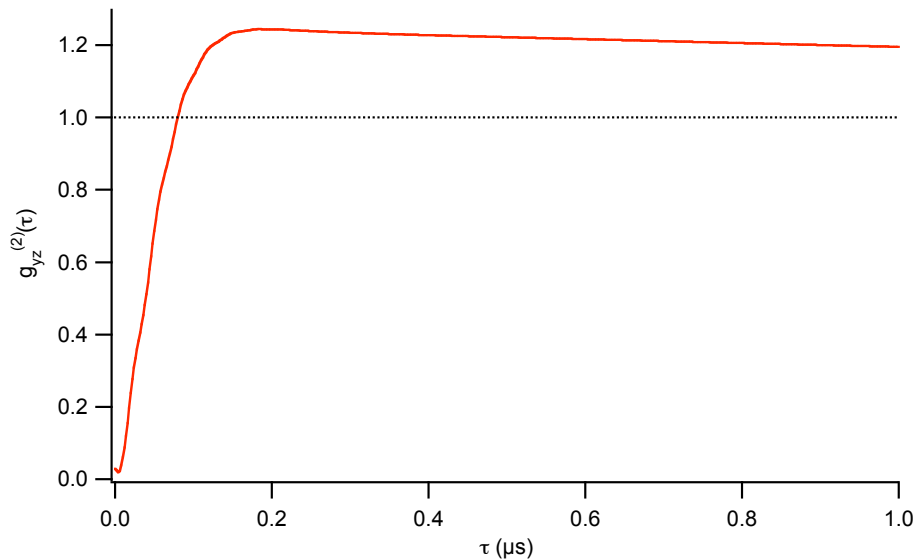
FIG. 6: Theoretical result for $g_{yz}^{(2)}(\tau)$ versus τ with parameters as in Fig. 5. The probe strength is such that the resonant intracavity photon number of the bare cavity would be 0.21 as in the experiment of Ref. [1]. The blue dotted line indicates $g^{(2)}(0) = 1$ for Poissonian statistics. This calculation was performed with a Fock basis of $\{0, 1, 2\}$ photons in the $\hat{z}$ polarized mode and $\{0, 1\}$ photons in the $\hat{y}$ polarized mode.

of Ref. [1], $g_{yz}^{(2)}(0) = 0.13 \pm 0.11$. Note that we have previously reported measurements of T_{zz} and made detailed comparisons with the theory described here [24].

In Fig. 6, we present the theoretical prediction for $g_{yz}^{(2)}(\tau)$ including the effects of Stark shifts and birefringence. We find that $g_{yz}^{(2)}(\tau)$ rises to unity at $\tau \simeq 80$ ns, well above the experimental result of $\tau \simeq 45$ ns. The theory, however, does not take into account atomic motion, but rather assumes the atom to be fixed at a place of optimal coupling. Since atomic motion clearly has a large effect on $g_{yz}^{(2)}(\tau)$, as is evident in Fig. 4(b) of Ref. [1], we believe that this is the dominant cause of the discrepancy [25].

VI. DISCUSSION

From the point of view described in general terms in Section II and elaborated in more detail in Sections III-V, our work in Ref. [1] satisfies the criteria for photon blockade. As indicated by Fig. 1(a,b) of Ref. [1], the Jaynes-Cummings ladder provides a means to achieve the condition $t_2 < |t_1|^2$, with the consequence that the intensity correlation function $g^{(2)}(0) < 1$ as presented in Fig. 2 of Ref. [1] and in the previous sections. Note also that by tuning to a two-photon resonance, our calculations indicate that photon bunching $g^{(2)}(0) \gg 1$ could be achieved for our atom-cavity system with $(\omega_p \simeq \omega_0 \pm g_0/4)$, again in accord with an understanding based upon transmission coefficients t_n. Photon bunching for the standard Jaynes-Cummings ladder of Fig. 1(a) in Ref. [1] is likewise achieved by tuning to the two-photon resonance at $\omega_p \simeq \omega_0 \pm g_0/\sqrt{2}$.

Our criteria for photon blockade do not demand the preservation of coherence in the transformation from input to output. One way to express a requirement for coherence in terms of the generic model in Section II is that the output state should be of the form of Eq. (5), and not of the form

$$\rho_{out} \sim |0\rangle\langle 0| + |t_1 \alpha|^2 |1\rangle\langle 1| , \qquad (9)$$

with the coherent amplitude lost. However, our view is that either Eq (5) or Eq. (9) suffices and qualifies as photon blockade. In fact, in practice the latter case of Eq. (9) might be the more "useful" for the following reasons.

With reference to Fig. 8 in Ref. [9], note that there are various contributions to $g^{(2)}(0)$ as a function of the amplitude of the driving field [Eq. (11b) of Ref. [9]]. The authors point out that "The decomposition shows how the behavior of $g^{(2)}(0) \ldots$ can be interpreted as the effect of self-homodyning between the coherent and incoherent components of the intracavity field." For our initial experiments with relatively modest ratios $g/(\kappa, \gamma)$, our view is that this complex, phase-dependent interplay should be avoided since it makes the blockade effect more "fragile" (less robust) than is the

case for Eq. (9). Basically, one wants a situation where there is no need to balance a set of interference terms (as in Eq. (11b) of Ref. [9]), but rather a more "generic" requirement of the sort presented in Section II, namely $|t_n| < |t_1|^n$. Note that an interpretation of photon antibunching similar to that expressed in Ref. [9] can be given for single-atom resonance fluorescence, as was first analyzed by Carmichael [22]. However, in this case the "miracle" is that the terms always sum to give $g^{(2)}(0) = 0$ for any drive strength, which is not the case for an atom in a cavity [22].

Our calculations show that the mean value for the amplitude of the transmitted field with polarization orthogonal to that of the coherent state input is zero. So, there is not a sense in which the coherent amplitude of the input is rotated in polarization by the atom-cavity system in the transformation to the output. Nevertheless, the orthogonally polarized output field can exhibit quantum interference, with an example being the value $g^{(2)}_{yz}(0) \gg 1$ for $\omega_p = \omega_0$ in Figs. 2, 5, which is presumably associated with the quantum state reduction and interference described by Carmichael and coworkers [13, 21], with here $g^{(2)}_{yz}(0) \simeq g^{(2)}_{zz}(0)$ for $\omega_p = \omega_0$.

For our experiment with multiple Zeeman states in the ground and excited levels and with two orthogonally polarized cavity modes (y, z), the eigenstates that are being driven for excitation along y with $\omega_p = \omega_0 \pm g_0$ are complex superpositions of various atomic Zeeman states and field states for the (y, z) polarizations. These eigenstates are entangled, so it is perhaps not surprising that examination of a particular component (e.g., for the field or atomic coherences) results in a mixed state with mean zero. Hence, many coherences for a single degree of freedom may vanish not because of dissipation *per se*, but rather because of entanglement with other components. Although we have not explored this question in detail, we think that this may explain why the mean amplitude for the transmitted z field is zero for excitation along y, as is the case for our results in Figs. 2, 5.

A final perspective to offer is to extend the discussion from the case with continuous excitation as has been implicit above to the case of pulsed excitation, as in Fig. 4 of Ref. [2]. Assume a pulse with duration short compared to any time scale associated with the "black box" described in Section II. For resonance fluorescence, consider a π pulse with duration $\tau_p \ll \gamma^{-1}$, so that there is now no coherent component for the fluorescent light for times $t > \tau_p$. In this case, resonance fluorescence would no longer satisfy the criterion for the preservation of coherence (as is the case for weak cw excitation [26]), yet it would still be perfectly antibunched. For the case of our atom-cavity system, we would require $g_0^{-1} \ll \tau_p \ll \kappa^{-1}$, in which case we would presumably obtain single photons on a pulse-by-pulse basis for the transmitted field with polarization orthogonal to that of the drive field, again with no preservation of coherence, which is presumably also true for EIT schemes in the limit of short pulses for the excitation [2, 6, 7, 8, 9]. Note that in either of these cases, the efficiency for the transformation of the pulsed driving field to a single photon at the output is necessarily small because of the mismatch of bandwidths, $\tau_p \ll \kappa^{-1}$.

VII. ACKNOWLEDGEMENTS

[1] K. M. Birnbaum, A. Boca, R. Miller, A. D. Boozer, T. E. Northup, and H. J. Kimble, Nature **436**, 87 (2005).
[2] A. Imamoḡlu, H. Schmidt, G. Woods, and M. Deutsch, Phys. Rev. Lett. **79**, 1467 (1997).
[3] T. A. Fulton and G. J. Dolan, Phys. Rev. Lett. **59**, 109 (1987).
[4] M. A. Kastner, Rev. Mod. Phys. **64**, 849 (1992).
[5] For a review, see K. K. Likharev, Proc. IEEE **87**, 606 (1999).
[6] P. Grangier, D. F. Walls, and K. M. Gheri, Phys. Rev. Lett. **81**, 2833 (1998).
[7] M. J. Werner and A. Imamoḡlu, Phys. Rev. A **61**, 011801 (1999).
[8] S. Rebić, S. M. Tan, A. S. Parkins, and D. F. Walls, J. Opt. B **1**, 490 (1999).
[9] S. Rebić, A. S. Parkins, and S. M. Tan, Phys. Rev. A **65**, 043806 and 063804 (2002).
[10] J. Kim, O. Bensen, H. Kan, and Y. Yamamoto, Nature **397**, 500 (1999).
[11] I. I. Smolyaninov, A. V. Zayats, A. Gungor, and C. C. Davis, Phys. Rev. Lett. **88**, 187402 (2002).
[12] L. Tian and H. J. Carmichael, Phys. Rev. A **46**, R6801 (1992).
[13] R. J. Brecha, P. R. Rice, and M. Xiao, Phys. Rev. A **59**, 2392 (1999).
[14] C. J. Hood, Doctoral Disertation (California Institute of Technology, 2000), Section 6.2.
[15] E. T. Jaynes and F. W. Cummings, Proc. IEEE **51**, 89 (1963).
[16] H. J. Kimble, Physica Scripta **T76**, 127 (1998).
[17] K. M. Birnbaum, A. Boca, R. Miller, A. D. Boozer, T. E. Northup, and H. J. Kimble, Nature Supplementary Information *http://www.nature.com/nature/journal/v436/n7047/suppinfo/nature03804.html* (2005).

[18] H. J. Kimble, M. Dagenais, and L. Mandel, Phys. Rev. Lett. **39**, 691 (1977).

[19] For a field with intensity operator $\hat{I}(t)$, $g^{(2)}(\tau) \equiv \langle : \hat{I}(t)\hat{I}(t+\tau) : \rangle / \langle : \hat{I}(t) : \rangle \langle : \hat{I}(t+\tau) : \rangle$, where the colons denote time and normal ordering [26].

[20] $T(\omega_p)$ is proportional to the ratio of photon flux $\langle \mathcal{E}_t^\dagger \mathcal{E}_t \rangle$ transmitted by M_2 to the flux $|\mathcal{E}_p|^2$ incident upon M_1, and normalized such that a cavity without an atom has a resonant transmission of unity. T_{zz} (T_{yz}) is proportional to the transmitted field polarized along $\hat{z}$ for an incident probe field polarized along $\hat{z}$ ($\hat{y}$). $g_{zz}^{(2)}$ ($g_{yz}^{(2)}$) is the intensity correlation function of the transmitted field polarized along $\hat{z}$ for an incident probe field polarized along $\hat{z}$ ($\hat{y}$).

[21] H. J. Carmichael, R. J. Brecha, and P. R. Rice, Opt. Commun. **82**, 73 (1991).

[22] H. J. Carmichael, Phys. Rev. Lett. **55**, 2790 (1985).

[23] J. McKeever *et al.*, Phys. Rev. Lett. **90**, 133602 (2003).

[24] A. Boca, R. Miller, K. M. Birnbaum, A. D. Boozer, J. McKeever, and H. J. Kimble, Phys. Rev. Lett. **93**, 233603 (2004).

[25] F. Diedrich and H. Walther, Phys. Rev. Lett. **58**, 203 (1987).

[26] *Optical Coherence and Quantum Optics*, L. Mandel and E. Wolf (Cambridge University Press, 1995).